

# Mechanical Modeling and Simulation of Ferromagnetic Fe Particle-Reinforced Elastomer Composites for Automotive Applications

Sponsor: National Science Foundation (Lizhi Sun, J.S. Chen)

## Objectives

This project includes three parts:

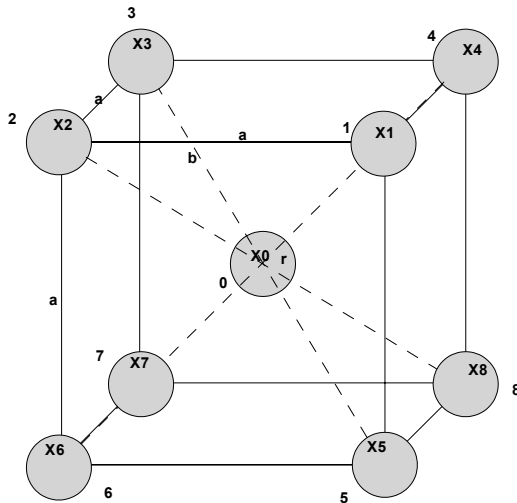
1. Micromechanics-based effective hyper-elastic constitutive laws for magnetostrictive particle-reinforced elastomer composites;
2. Numerical simulations of composite unit cell using meshfree method to determine constitutive coefficients of composites; and
3. Large-scale model-based structural meshfree simulations of engine mounts to demonstrate the proposed model capacity for the structural responses.

## Results

1. A new model of effective constitutive relations for magnetostrictive particle-reinforced elastomer composites has been proposed based on a micromechanics approach. Magnetostrictive spherical particles are assumed to be elastic. The effects of magnetic fields have been treated using the prescribed Eshelby-type transferred eigenstrains acting on those particles. A split of effective free energy of composites is proposed as

$$W = (1 - \phi)W_m + \phi W_p$$

based on the fact that particles and the matrix deform simultaneously under the external loading and applied magnetic field. From the unit cell model shown in Figure 1, the respective elastic energies of particles and matrix can be obtained as:



$$W_m = \frac{nk\Theta}{6} \int_{I_1^0}^{I_1} I_1 \ell^{-1} \left[ \frac{I_1^{1/2}}{\sqrt{3N}} \right] \frac{\sqrt{3N}}{I_1^{1/2}} dI_1$$

$$W_p = \mu_p \chi_1^2 \left( \ln^2 \frac{\lambda_1}{\lambda_1^0} + \ln^2 \frac{\lambda_2}{\lambda_2^0} + \ln^2 \frac{\lambda_3}{\lambda_3^0} \right)$$

Figure 1. Unit-cell model of magnetostrictive particle-reinforced elastomer composites.

Therefore, the effective hyperelastic constitutive law can be written as

$$\sigma_i = \lambda_I \frac{\partial W}{\partial \lambda_I} + p$$

where  $\sigma_i$ ,  $p$ , and  $\lambda_I$  denote the principal Cauchy stress, hydrostatic pressure, and principal stretch of composites, respectively. Comparison with experimental data is shown in Figure 2.

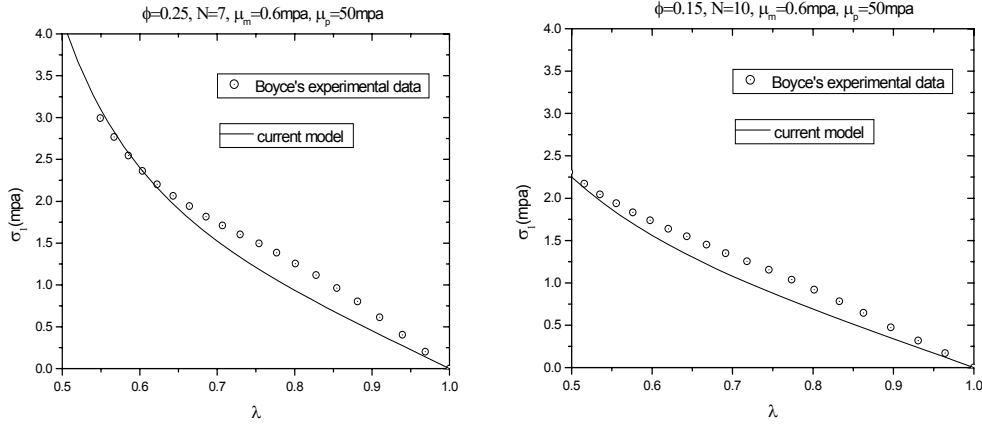


Figure 2. Comparisons between the present model and experimental data on hyperelastic responses of elastomer composites.

- Unit cell computational micromechanics model is used to determine the effective constitutive equations of the composites. It is well known that the finite element method is ineffective in modeling material interfaces due to the difficulties in matching meshes with different mesh densities along the material interface. In this research, a meshfree method is developed to resolve the discretization difficulties and to perform adaptive local refinement for desired resolution near material interfaces in the unit cell. Nevertheless, our earlier development of meshfree method based on the reproducing kernel particle method (RKPM) cannot capture the discontinuity of strain or heat flux across the composite material interface. For this reason, a generalized reproducing kernel approximation of displacement  $u(x)$  (or temperature) is proposed as follows:

$$u^h(\mathbf{x}) = \sum_I \Psi_I(\mathbf{x}) u_I$$

Here  $\Psi_I(\mathbf{x})$  is the shape function that contains two parts

$$\Psi_I(\mathbf{x}) = \hat{\Psi}_I(\mathbf{x}) + \bar{\Psi}_I(\mathbf{x})$$

where  $\hat{\Psi}_I(\mathbf{x})$  is a primitive function used to introduce Kronecker delta properties and desired smoothness in the approximation, and  $\bar{\Psi}_I(\mathbf{x})$  is an enrichment function for imposing n-th order reproducing conditions:

$$\bar{\Psi}_l(\mathbf{x}) = \mathbf{H}^T(\mathbf{x} - \mathbf{x}_l) \Phi_a(\mathbf{x} - \mathbf{x}_l) \mathbf{a}(\mathbf{x})$$

where  $\mathbf{H}^T(\mathbf{x} - \mathbf{x}_l) = [1, x_1 - x_{1l}, x_2 - x_{2l}, x_3 - x_{3l}, (x_1 - x_{1l})^2, \dots, (x_3 - x_{3l})^n]$  is a vector of  $n$ -th order basis functions,  $\Phi_a(\mathbf{x} - \mathbf{x}_l)$  is the kernel that defines the locality of the approximation, and  $\mathbf{a}(\mathbf{x})$  is a coefficient vector obtained from the following reproducing conditions:

$$\sum_I [\hat{\Psi}_I(\mathbf{x}) + \bar{\Psi}_I(\mathbf{x})] x_{1l}^i x_{2l}^j x_{3l}^k = x_1^i x_2^j x_3^k; \quad 0 \leq i + j + k \leq n$$

In this study, the primitive function is introduced as a function which has discontinuous derivative at specified locations and direction, while maintaining continuous derivative elsewhere. A one-dimensional example is shown as follows:

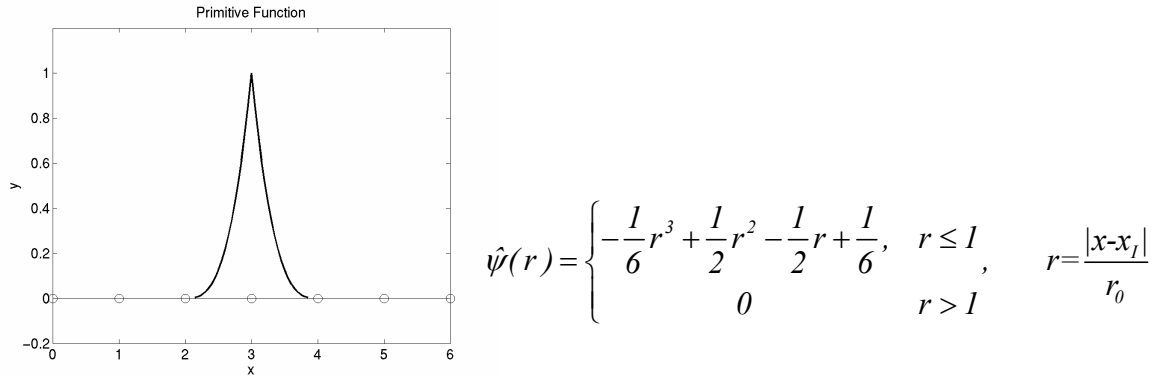


Figure 3 One dimensional primitive function with discontinuous derivative

By introducing this primitive function at the location with material discontinuity, the resulting meshfree shape function has derivative discontinuity at the specified location and continuous derivative elsewhere. This formulation procedure is illustrated in Fig 4.

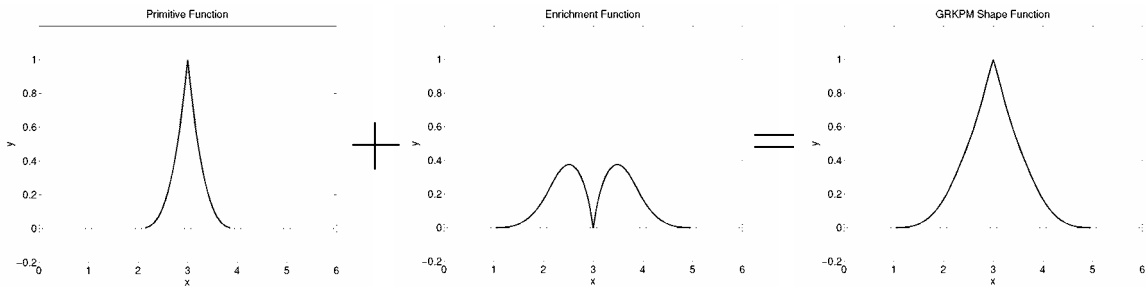


Figure 4 The  $C^0$  generalized reproducing kernel shape function

This new meshfree method is called the interface enriched reproducing kernel particle method (I-RKPM). A heat conduction of a bi-material with a circular inclusion is analyzed. The problem geometry and discretization using finite element and the proposed I-RKPM are shown in Fig. 5. Note that in the finite element discretization, the mesh is generated with

geometry confinement. On the other hand, a non-restrictive discretization is can be easily generated for I-RKPM. A very refined finite element model is used to serve as a reference solution for verification of meshfree solution.

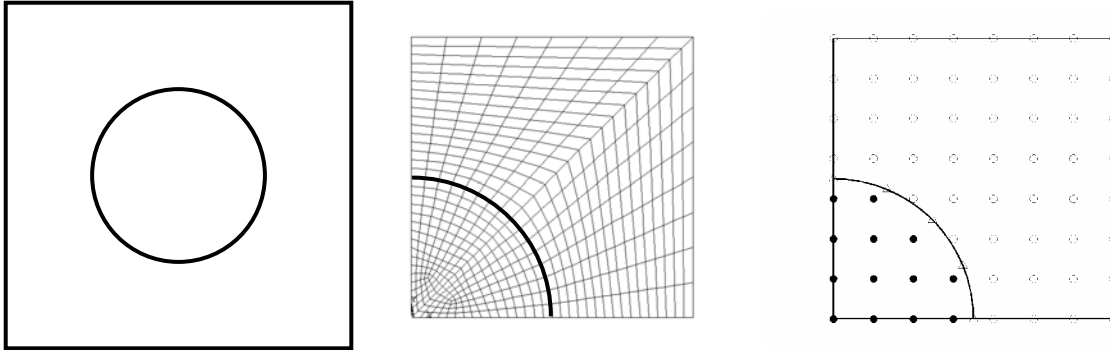


Figure 5 Problem Geometry and Finite Element and Meshfree Discretization

The strain distribution across the normal direction of material interface predicted by the finite element method (FEM), the reproducing kernel particle method (RKPM), and the new interface enriched reproducing kernel particle method (I-RKPM) are compared in Fig. 6. The results show a significant improvement of the new I-RKPM over the conventional meshfree RKPM.

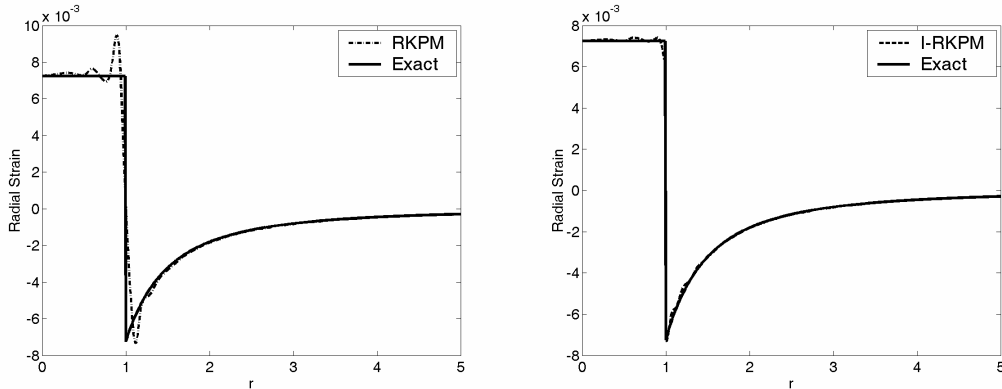


Figure 6 Temperature and its gradient along the diagonal direction

First the tension response of Magnetostrictive Particle Filled Elastomer (MPFE) is analyzed. To evaluate the effect of mangnetostritive eigen-strain to the response of MPFE, various degrees of magnetostrictive eigen-strain, ranging from 1 to 10 percent, are considered. The local fluctuating deformation and overall combined deformation field for the case with a 3 percent magnetostrictive eigen-strain are plotted in figure 7. The responses of homogenized axial Cauchy stress versus axial stretch are shown in figure 13. Although the deformations for both cases look similar, figure 8 shows that magnetostrictive eigen-strain does influence the overall tension response of MPFE. The shear defoemation of MPFE is also shown in Fig. 9.



Figure 7 Displacement fields with 3% magnetostrictive eigen-strain for tension test: (a) Local fluctuating deformation; (b) Microscopic total deformation

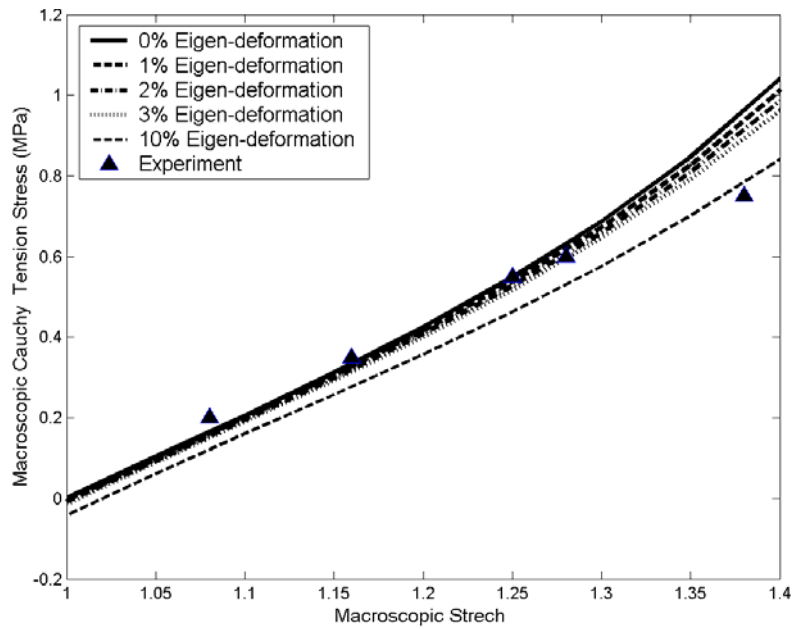


Figure 8 Axial Cauchy stress versus axial stretch

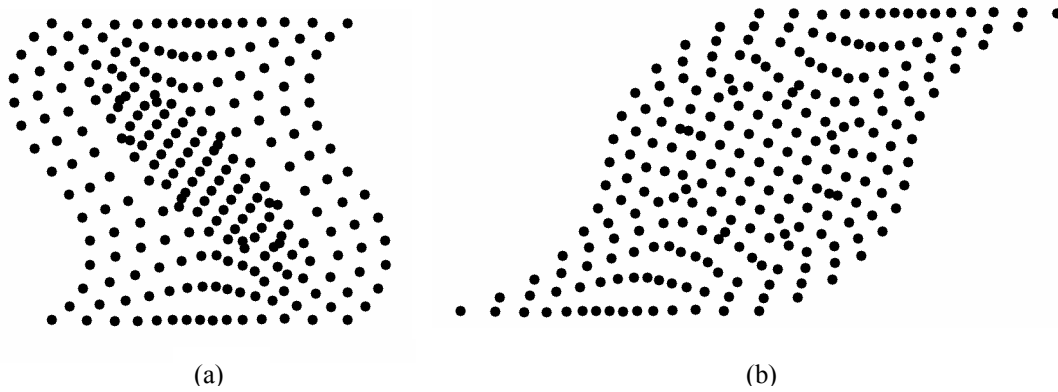


Figure 9 Displacement fields without magnetostrictive eigen-strain effect for simple shear test:  
(a) Local fluctuating deformation; (b) Microscopic total deformation